



Queensland University of Technology
Brisbane Australia

This is the author's version of a work that was submitted/accepted for publication in the following source:

Frost, Ray L., Palmer, Sara J., Henry, Dermot A., & Pogson, Ross (2011) A Raman spectroscopic study of the 'cave' mineral ardealite $\text{Ca}_2(\text{HPO}_4)(\text{SO}_4)\cdot 4\text{H}_2\text{O}$. *Journal of Raman Spectroscopy*, 42(6), pp. 1447-1454.

This file was downloaded from: <http://eprints.qut.edu.au/42037/>

© Copyright 2011 John Wiley & Sons, Ltd.

Notice: *Changes introduced as a result of publishing processes such as copy-editing and formatting may not be reflected in this document. For a definitive version of this work, please refer to the published source:*

<http://dx.doi.org/10.1002/jrs.2855>

A Raman spectroscopic study of the 'cave' mineral ardealite $\text{Ca}_2(\text{HPO}_4)(\text{SO}_4)\cdot 4\text{H}_2\text{O}$

Ray L. Frost,¹• Sara J. Palmer,¹ Dermot A. Henry² and Ross Pogson²

¹Chemistry Discipline, Faculty of Science and Technology, Queensland University of Technology, GPO Box 2434, Brisbane Queensland 4001, Australia.

²Museum Victoria, Geosciences, GPO box 666, Melbourne 3001

³Mineralogy & Petrology, Australian Museum, 6 College St., Sydney, NSW, Australia 2010

Abstract

The mineral ardealite $\text{Ca}_2(\text{HPO}_4)(\text{SO}_4)\cdot 4\text{H}_2\text{O}$ is a 'cave' mineral and is formed through the reaction of calcite with bat guano. The mineral shows disorder and the composition varies depending on the origin of the mineral. Raman spectroscopy complimented with infrared spectroscopy has been used to characterise the mineral ardealite. The Raman spectrum is very different from that of gypsum. Bands are assigned to SO_4^{2-} and HPO_4^{2-} stretching and bending modes.

Keywords: Raman spectroscopy, phosphate, sulphate, ardealite

Introduction

• Author to whom correspondence should be addressed (r.frost@qut.edu.au)

33 The mineral ardealite is known as a cave mineral and has been found in many caves
34 worldwide ¹⁻⁶. Phosphates have been known to exist in the Jenolan caves for a very long time
35 ⁷⁻⁹. Dating of clays in these caves suggest the caves are very old around 350 million years ¹⁰.
36 The mineral is a mixed anion sulphate phosphate of calcium and is formed by the reaction of
37 bat guano with calcite. The mineral is monoclinic of point group *m* and forms very thin platy
38 crystals or powdery crusts. The mineral is intimately associated with brushite and gypsum.
39 The formula of the mineral is given as $\text{Ca}_2(\text{HPO}_4)(\text{SO}_4)\cdot 4\text{H}_2\text{O}$ but the composition of the
40 mineral can vary according to the cave of origin. The mineral is often yellowish probably
41 due to the presence of iron in the mineral composition.

42

43 Raman spectroscopy has proven very useful for the study of minerals ¹¹⁻²⁴. Indeed Raman
44 spectroscopy has proven most useful for the study of diagenetically related minerals as often
45 occurs with minerals containing sulphate and phosphate groups. This paper is a part of
46 systematic studies of vibrational spectra of minerals of secondary origin in the oxide
47 supergene zone. In this work we attribute bands at various wavenumbers to vibrational modes
48 of ardealite using Raman spectroscopy and relate the spectra to the structure of the mineral.

49

50 **Experimental**

51

52 **Minerals**

53 The mineral ardealite was sourced from two sources namely (a) The Australian Museum and
54 originated from the Jenolan caves, New South Wales, Australia and (b) from Museum
55 Victoria where the ardealite mineral originated from Moorba Cave, Jurien Bay, Western
56 Australia, Australia. The mineral has been analysed and the data published ²⁵.

57

58 **Raman spectroscopy**

59

60 Crystals of ardealite were placed on a polished metal surface on the stage of an Olympus
61 BHSM microscope, which is equipped with 10x, 20x, and 50x objectives. The microscope is
62 part of a Renishaw 1000 Raman microscope system, which also includes a monochromator, a
63 filter system and a CCD detector (1024 pixels). The Raman spectra were excited by a
64 Spectra-Physics model 127 He-Ne laser producing highly polarised light at 633 nm and
65 collected at a nominal resolution of 2 cm^{-1} and a precision of $\pm 1\text{ cm}^{-1}$ in the range between
66 100 and 4000 cm^{-1} . Repeated acquisition on the crystals using the highest magnification (50x)

67 was accumulated to improve the signal to noise ratio in the spectra. Spectra were calibrated
68 using the 520.5 cm^{-1} line of a silicon wafer.

69

70 **Infrared spectroscopy**

71

72 Infrared spectra were obtained using a Nicolet Nexus 870 FTIR spectrometer with a smart
73 endurance single bounce diamond ATR cell. Spectra over the $4000\text{--}525\text{ cm}^{-1}$ range were
74 obtained by the co-addition of 64 scans with a resolution of 4 cm^{-1} and a mirror velocity of
75 0.6329 cm/s . Spectra were co-added to improve the signal to noise ratio.

76

77 Band component analysis was undertaken using the Jandel 'Peakfit' (Erkrath,
78 Germany) software package which enabled the type of fitting function to be selected and
79 allowed specific parameters to be fixed or varied accordingly. Band fitting was done using a
80 Lorentz-Gauss cross-product function with the minimum number of component bands used
81 for the fitting process. The Lorentz-Gauss ratio was maintained at values greater than 0.7 and
82 fitting was undertaken until reproducible results were obtained with squared correlations (r^2)
83 greater than 0.995. Band fitting of the spectra is quite reliable providing there is some band
84 separation or changes in the spectral profile.

85 **Results and discussion**

86

87 ***Background***

88

89 The Raman spectroscopy of the aqueous sulphate tetrahedral oxyanion yields the
90 symmetric stretching (ν_1) vibration at 981 cm^{-1} , the in-plane bending (ν_2) mode at 451 cm^{-1} ,
91 the antisymmetric stretching (ν_3) mode at 1104 cm^{-1} and the out-of-plane bending (ν_4) mode
92 at 613 cm^{-1} ²⁶. Ross reports the interpretation of the infrared spectra for potassium alum as
93 ν_1 , 981 cm^{-1} ; ν_2 , 465 cm^{-1} ; ν_3 , $1200, 1105\text{ cm}^{-1}$; ν_4 , 618 and 600 cm^{-1} ²⁷. Water stretching
94 modes were reported at 3400 and 3000 cm^{-1} , bending modes at 1645 cm^{-1} , and librational
95 modes at 930 and 700 cm^{-1} ²⁸. The Raman spectrum of the mineral chalcantite shows a
96 single symmetric stretching mode at 984.7 cm^{-1} . Two ν_2 modes are observed at 463 and 445
97 cm^{-1} and three ν_3 modes at $1173, 1146$ and 1100 cm^{-1} . The ν_4 mode is observed as a single
98 band at 610 cm^{-1} . A complex set of overlapping bands is observed in the low wavenumber

99 region at 257, 244, 210 136 and 126 cm^{-1} . Recently, Raman spectra of four basic copper
100 sulphate minerals, namely antlerite, brochantite, posnjakite and langite, were published²⁹.
101 The SO symmetric stretching modes for the four basic copper sulphate minerals are observed
102 at 985, 990, 972 and 974 cm^{-1} . Only the mineral brochantite showed a single band in this
103 region. Multiple bands were observed for these minerals in the antisymmetric stretching
104 region. Some sulphates have their symmetry reduced through acting as monodentate and
105 bidentate ligands³⁰. In the case of bidentate behaviour both bridging and chelating ligands
106 are known. This reduction in symmetry is observed by the splitting of the ν_3 and ν_4 into two
107 components under C_{3v} symmetry and 3 components under C_{2v} symmetry. Raman spectra of
108 hydrogen phosphate oxyanions show a symmetric stretching mode (ν_1) at $\sim 860 \text{ cm}^{-1}$, the
109 antisymmetric stretching mode (ν_3) at $\sim 1150 \text{ cm}^{-1}$, the symmetric bending mode (ν_2) at ~ 460
110 cm^{-1} and the ν_4 mode at $\sim 590 \text{ cm}^{-1}$.

111

112 ***Raman Spectroscopy***

113

114 Raman spectroscopy is a very powerful tool for the analysis of the molecular structure
115 of minerals especially minerals containing oxyanions. The Raman spectrum of ardealite from
116 the two sources in the 800 to 1200 cm^{-1} is shown in Fig. 1. There appears to be two
117 overlapping bands at around 998 and 1002 cm^{-1} . These bands are assigned to the $\nu_1 \text{SO}_4^{2-}$
118 stretching mode. In the white material from the Jenolan caves, attributed to gypsum an
119 intense Raman band is observed at 1008 cm^{-1} (Fig. S1). The band is perfectly symmetric and
120 not asymmetric as occurs in the Raman spectrum of ardealite. It is suggested that there are
121 two non-equivalent sulphate units in the ardealite structure. Alternatively a band from the
122 sulphate and hydrogen phosphate anions overlaps. The low intensity Raman band at 1140
123 cm^{-1} is assigned to the $\nu_3 \text{SO}_4^{2-}$ antisymmetric stretching modes. A band occurs for gypsum
124 at 1139 cm^{-1} . A second Raman band is observed for the ardealite for the sample D49535 at
125 1102 cm^{-1} . One possibility is that this band is assignable to the $\nu_3 \text{HPO}_4^{2-}$ antisymmetric
126 stretching mode. The band is not observed in the Raman spectrum of gypsum. The Raman
127 spectrum of the phosphate mineral newberyite has been reported³¹. Raman bands were
128 observed at 1154 and 1195 cm^{-1} .

129

130 A Raman band is found at 862 cm^{-1} for ardealite. This band is assigned to the $\nu_1 \text{HPO}_4^{2-}$
131 symmetric stretching mode. The band is due to the presence of hydrogen phosphate units in

132 the ardealite structure. The band is not observed in the Raman spectrum of gypsum. A Raman
133 band was observed in the spectrum of newberyite $\text{Mg}(\text{PO}_3\text{OH})\cdot 3\text{H}_2\text{O}$ at 887 cm^{-1} and was
134 attributed to HPO_4^{2-} symmetric stretching mode³¹. Such bands are normally intense in the
135 infrared spectrum but of low intensity in the Raman spectrum. Rajendran and Keefe³²
136 studied the growth and characterisation of calcium hydrogen phosphate dihydrate and
137 reported the FTIR and Raman spectra. These researchers observed a band at 875 cm^{-1} and
138 assigned this band to the HPO_4^{2-} POP antisymmetric stretching mode. However this
139 assignment differs from our interpretation. Soptrajanov *et al.*³³ reported the FT-IR and
140 Raman spectra of a manganese hydrogen phosphate trihydrate and assigned an observed band
141 at 889 cm^{-1} to a P-O(H) stretching vibration. These workers showed that the band was
142 deuterium sensitive.

143

144 The Raman spectra of ardealite in the 350 to 700 cm^{-1} region are shown in Fig. 2. For the
145 ardealite from WA, a Raman band is found at 610 cm^{-1} . This band is assigned to the ν_4
146 $(\text{SO}_4)^{2-}$ bending modes. In the Raman spectrum of the NSW sample, Raman bands are found
147 at 598 , 613 and 670 cm^{-1} and are assigned to this vibrational mode. The intense Raman band
148 at 502 cm^{-1} for the WA sample and at 505 and 528 cm^{-1} for the NSW sample are assigned to
149 the $\nu_4(\text{HPO}_4)^{2-}$ bending modes. The mineral newberyite $\text{Mg}(\text{PO}_3\text{OH})\cdot 3\text{H}_2\text{O}$ also contains a
150 hydrogen phosphate anion. The Raman spectrum of this mineral has been reported³¹. An
151 intense band was observed for this mineral at 498 cm^{-1} . Rajendran and Keefe³² reported
152 Raman bands at 521 and 586 cm^{-1} and assigned these bands to (H-O)P=O absorption bands.
153 This assignment is in contrast to the assignment of bands by Farmer³⁴. The Raman bands at
154 421 and 448 cm^{-1} (NSW) and 418 and 453 cm^{-1} (WA) are assigned to the $\nu_2(\text{SO}_4)^{2-}$ bending
155 modes. The Raman band at 363 cm^{-1} (both NSW and WA) is assigned to the $\nu_2(\text{HPO}_4)^{2-}$
156 bending mode. In the Raman spectrum of gypsum (Fig. S2), no bands are found at 502 and
157 363 cm^{-1} . Raman bands for gypsum are observed at 415 , 494 , 620 and 671 cm^{-1} . Raman
158 spectra in the low wavenumber region are shown in Fig. 3. It is considered that these bands
159 in this spectral region are associated with water hydrogen bonded to the sulphate and
160 phosphate anions. There is a resemblance to the Raman spectrum of gypsum in this spectral
161 region (Fig. S3). A Raman spectrum of gypsum in the OH stretching region is given in Fig.
162 S4. However it was not possible to obtain a Raman spectrum of ardealite in this spectral
163 region. This is attributed to the poor crystallinity of the mineral sample and the fact that water
164 has a very poor Raman scattering cross section.

165

166 **Infrared Spectroscopy**

167

168 The infrared spectra of the two ardealite minerals in the 900 to 1300 cm^{-1} region are
169 displayed in Fig. 4. The infrared band at 998 cm^{-1} (NSW) and 995 cm^{-1} (WA) are assigned
170 to the infrared forbidden $(\text{SO}_4)^{2-}$ stretching vibration. The band has become activated because
171 of the reduction in symmetry of the sulphate/phosphate anion. It is thought that coupling
172 occurs between the sulphate and phosphate vibrations resulting in the observation of a single
173 asymmetric band. The infrared band at $\sim 1093 \text{ cm}^{-1}$ is assigned to the $(\text{HPO}_4)^{2-} \nu_3$
174 antisymmetric stretching vibration. The series of bands at 1131, 1147, 1171 cm^{-1} (NSW) and
175 1130, 1148 and 1179 cm^{-1} are attributed to the $(\text{SO}_4)^{2-} \nu_3$ antisymmetric stretching vibrations.
176 The observation of multiple ν_3 bands supports the concept of a reduction in symmetry of the
177 sulphate anion. The Raman spectrum of gypsum is very different in this spectral region (Fig.
178 S5). Farmer³⁴ reported infrared bands at 948, 1068 and 1150 cm^{-1} for Na_2HPO_4 and
179 assigned these bands to the $(\text{HPO}_4)^{2-} \nu_3$ antisymmetric stretching vibrations.
180 Soptrajanov et al.³³ for manganese hydrogen phosphate trihydrate reported infrared bands at
181 971, 1035, 1135 and 1154 cm^{-1} and assigned these bands to PO_3 stretching vibrations.

182

183 The infrared spectra of ardealite in the 550 to 900 cm^{-1} region are reported in Fig. 5. Intense
184 infrared bands are observed at $\sim 862 \text{ cm}^{-1}$. The band is asymmetric in the infrared spectrum
185 of the NSW sample. This band is assigned to the $(\text{HPO}_4)^{2-} \nu_1$ symmetric stretching mode.
186 Farmer³⁴ tabulated the band positions of minerals containing the hydrogen phosphate anion
187 (Table 17 III page 386). In this work, the infrared band at 860 cm^{-1} was described as the
188 $(\text{HPO}_4)^{2-} \nu_1$ symmetric stretching mode.

189

190 The band at $\sim 670 \text{ cm}^{-1}$ is assigned to the infrared $\nu_4(\text{SO}_4)^{2-}$ bending modes. The strong
191 infrared band at $\sim 590 \text{ cm}^{-1}$ is assigned to the $\nu_4(\text{HPO}_4)^{2-}$ bending modes. Farmer³⁴ reported
192 the position of bands attributed to $(\text{HPO}_4)^{2-}$ bending vibrations. These bands are observed in
193 the 520 to 590 cm^{-1} spectral region. The $\nu_2(\text{HPO}_4)^{2-}$ bending modes are found below 500
194 cm^{-1} which is below the limits of the infrared spectrometer. These infrared bands are found
195 at ~ 430 to 460 cm^{-1} range.

196

197 The infrared spectra of ardealite in the 1400 to 1800 cm^{-1} region are reported in Fig. 6. This
198 spectral region is where the water bending vibration is found. The spectrum for the NSW
199 sample shows complexity with infrared bands observed at 1619, 1653 and 1683 cm^{-1} . The
200 position of these bands supports the concept that water is in different environments in the
201 structure of ardealite. The band at 1619 cm^{-1} is due to weakly hydrogen bonded water. The
202 bands at 1653 and 1683 cm^{-1} are attributed to strongly hydrogen bonded water molecules. In
203 the infrared spectrum of the WA mineral, infrared bands are observed at 1604, 1651, 1684
204 cm^{-1} . In the infrared spectrum of gypsum, two distinct and clearly resolved bands are
205 observed at 1619 and 1682 cm^{-1} (Fig. S7). Infrared bands observed at 1346 and 1439 cm^{-1}
206 (WA) and 1440 cm^{-1} (NSW) are assigned to POH in-phase deformation modes. The band
207 positions are in agreement with the position of POH bands reported by Farmer³⁴. The
208 infrared spectrum of ardealite in the 2600 to 3800 cm^{-1} region is shown in Fig. 7. The
209 spectral profile is complex with a series of overlapping bands. Infrared bands are resolved at
210 3026, 3160, 3257, 3333, 3405 and 3521 cm^{-1} for the NSW sample. The complexity of the
211 water stretching bands is in harmony with the water bending modes centred upon $\sim 1650 \text{ cm}^{-1}$.
212 The infrared spectrum of gypsum is very different (Fig. S8).

213

214 **Conclusions**

215

216 Raman complimented with infrared spectroscopy has been used to characterise the ‘cave’
217 mineral ardealite $\text{Ca}_2(\text{HPO}_4)(\text{SO}_4)\cdot 4\text{H}_2\text{O}$. The mineral is an unusual mineral from a chemistry
218 point of view as the mineral contains hydrogen phosphate and sulphate anions. The mineral
219 is formed by the reaction of phosphates from bat guano and calcite. The Raman and infrared
220 spectra reflect the composition of the mineral with bands attributed to H_2O , HPO_4 and SO_4
221 stretching and bending modes.

222

223 **Acknowledgements**

224

225 The financial and infra-structure support of the Queensland University of Technology
226 Chemistry Discipline of the Faculty of Science and Technology, is gratefully acknowledged.
227 The Australian Research Council (ARC) is thanked for funding the instrumentation.

228

229 **References**

230

231 [1] D.-G. Dumitras, S. Marincea, E. Bilal, F. Hatert, *Can. Min.* **2008**, *46*, 431-445.232 [2] C. A. Hill, *Cave Minerals*, 1976.233 [3] D. Moravansky, M. Orvosova, *Miner. Slov.* **2007**, *39*, 203-216.234 [4] D. Moravansky, P. Zenis, *Miner. Slov.* **1997**, *29*, 61-72.235 [5] B. P. Onac, J. E. Mylroie, W. B. White, *Carb.Evap.* **2001**, *16*, 8-16.236 [6] W. B. White, *Sci. Speleol.* **1976**, 267-327.237 [7] J. C. H. Mingaye, *Rept. Australian Assoc.* **1898**, *7*, 111-116.238 [8] J. C. H. Mingaye, *Records Geol. Survey N.S.W.* **1899**, *6*, 111-116.239 [9] C. A. Suessmilch, W. G. Stone, *J. Royal Soc. N.S.W.* **1916**, *49*, 332-384.240 [10] R. A. L. Osborne, H. Zwingmann, R. E. Pogson, D. M. Colchester, *Aust. J. Earth*241 *Sc.* **2006**, *53*, 377-405.242 [11] S. Bahfenne, R. L. Frost, *J. Raman Spectrosc.* **2010**, *41*, 329-333.243 [12] S. Bahfenne, R. L. Frost, *J. Raman Spectrosc.* **2010**, *41*, 465-468.244 [13] J. Cejka, S. Bahfenne, R. L. Frost, J. Sejkora, *J. Raman Spectrosc.* **2010**, *41*, 74-77.245 [14] J. Cejka, J. Sejkora, J. Plasil, S. Bahfenne, S. J. Palmer, R. L. Frost, *J. Raman*246 *Spectrosc.* **2010**, *41*, 459-464.247 [15] R. L. Frost, S. Bahfenne, *J. Raman Spectrosc.* **2010**, *41*, 207-211.248 [16] R. L. Frost, S. Bahfenne, *J. Raman Spectrosc.* **2010**, *41*, 325-328.249 [17] R. L. Frost, S. Bahfenne, J. Cejka, J. Sejkora, S. J. Palmer, R. Skoda, *J. Raman*250 *Spectrosc.* **2010**, *41*, 690-693.251 [18] R. L. Frost, S. Bahfenne, J. Cejka, J. Sejkora, J. Plasil, S. J. Palmer, *J. Raman*252 *Spectrosc.* **2010**, *41*, 814-819.253 [19] R. L. Frost, K. H. Bakon, S. J. Palmer, *J. Raman Spectrosc.* **2010**, *41*, 78-83.

- 254 [20] R. L. Frost, J. Cejka, J. Sejkora, J. Plasil, S. Bahfenne, S. J. Palmer, *J. Raman*
255 *Spectrosc.* **2010**, *41*, 571-575.
- 256 [21] R. L. Frost, J. Cejka, J. Sejkora, J. Plasil, S. Bahfenne, S. J. Palmer, *J. Raman*
257 *Spectrosc.* **2010**, *41*, 566-570.
- 258 [22] R. L. Frost, S. J. Palmer, L.-M. Grand, *J. Raman Spectrosc.* **2010**, *41*, 791-796.
- 259 [23] R. L. Frost, J. Sejkora, E. C. Keeffe, J. Plasil, J. Cejka, S. Bahfenne, *J. Raman*
260 *Spectrosc.* **2010**, *41*, 202-206.
- 261 [24] J. Sejkora, J. Cejka, R. L. Frost, S. Bahfenne, J. Plasil, E. C. Keeffe, *J. Raman*
262 *Spectrosc.* **2010**, *41*, 1038-1043.
- 263 [25] J. W. Anthony, R. A. Bideaux, K. W. Bladh, M. C. Nichols, Handbook of
264 Mineralogy, Mineral Data Publishing, Tuscon, Arizona, USA, 2000.
- 265 [26] R. L. Frost, P. A. Williams, W. Martens, J. T. Kloprogge, P. Leverett, *Journal of*
266 *Raman Spectroscopy* **2002**, *33*, 260-263.
- 267 [27] S. D. Ross, in *The infrared spectra of minerals*, **1974**, Chapter 18 pp 423, The
268 Mineralogical Society London.
- 269 [28] S. D. Ross, *Inorganic Infrared and Raman Spectra* (European Chemistry Series),
270 1972.
- 271 [29] W. Martens, R. L. Frost, J. T. Kloprogge, P. A. Williams, *Journal of Raman*
272 *Spectroscopy* **2003**, *34*, 145-151.
- 273 [30] R. L. Frost, J. T. Kloprogge, P. A. Williams, P. Leverett, *Journal of Raman*
274 *Spectroscopy* **2000**, *31*, 1083-1087.
- 275 [31] R. L. Frost, M. L. Weier, W. N. Martens, D. A. Henry, S. J. Mills, *Spectrochimic.*
276 *Acta*, **2005**, *62A*, 181-188.
- 277 [32] K. Rajendran, C. D. Keefe, *Cryst. Res. technol.* **2010**, *45*, 939-945.

- 278 [33] B. Soptrajanov, V. Stefov, I. Kuzmanovski, G. Jovanovski, *J. Molec. Struc.***1999**, 482-
279 483, 103-107.
- 280 [34] V. C. Farmer, Mineralogical Society Monograph 4: The Infrared Spectra of Minerals,
281 1974.
- 282
- 283
- 284

285

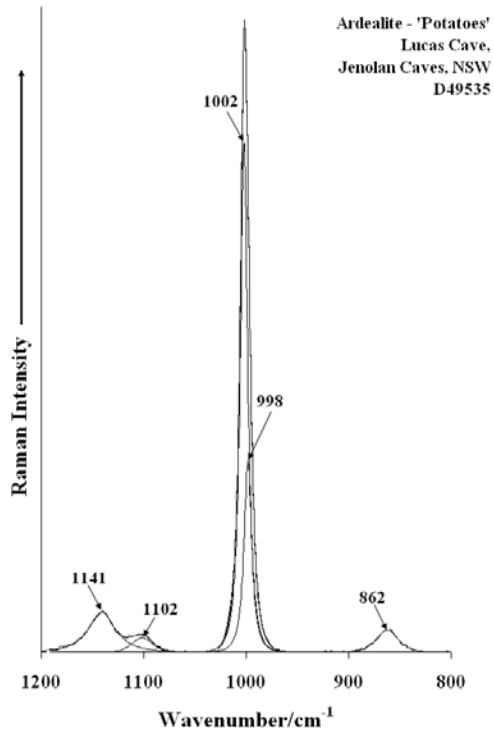


Figure 1a

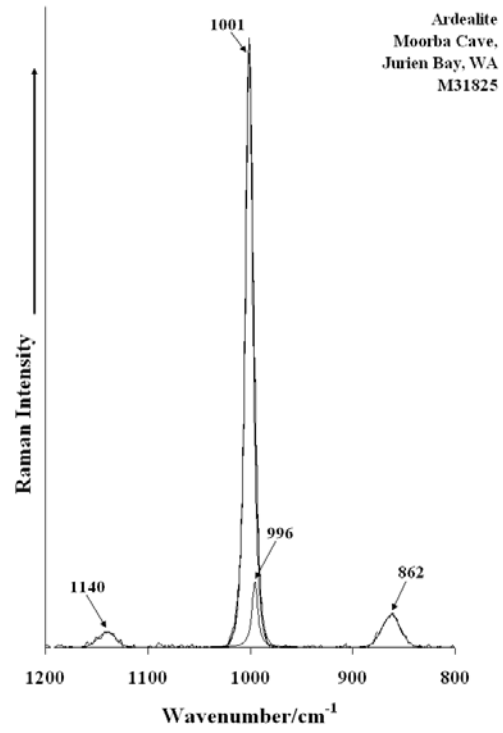


Figure 1b

286

287

288

289

290

291

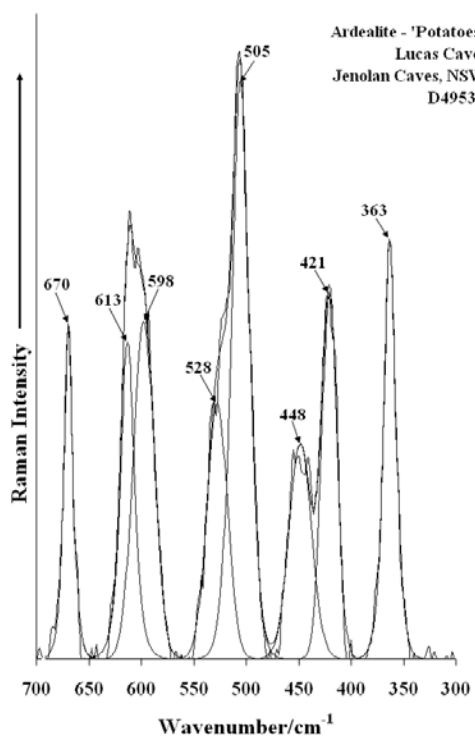


Figure 2a

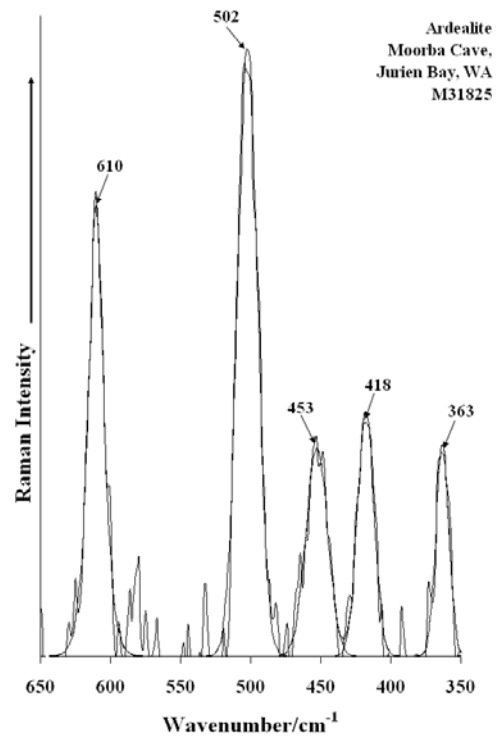


Figure 2b

292

293

294

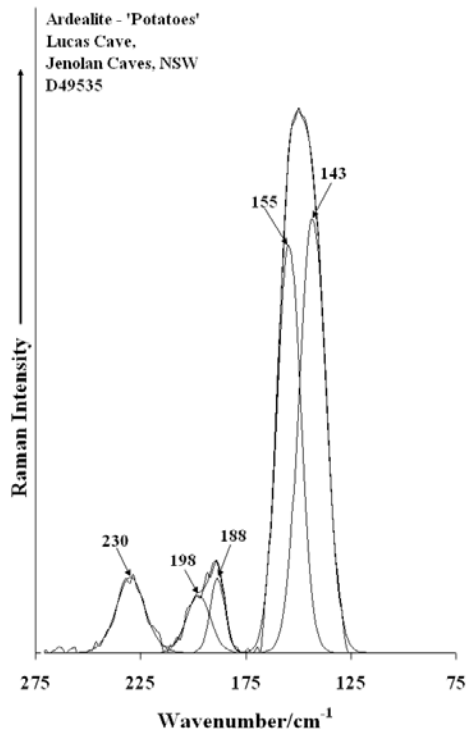


Figure 3a

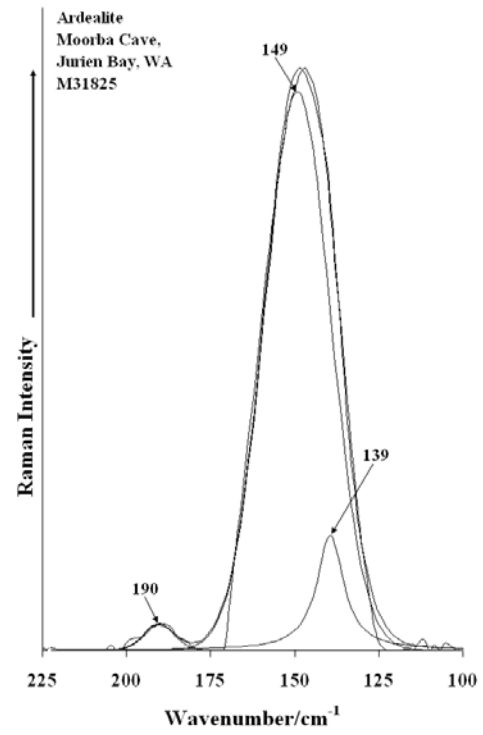


Figure 3a

295

296

297

298

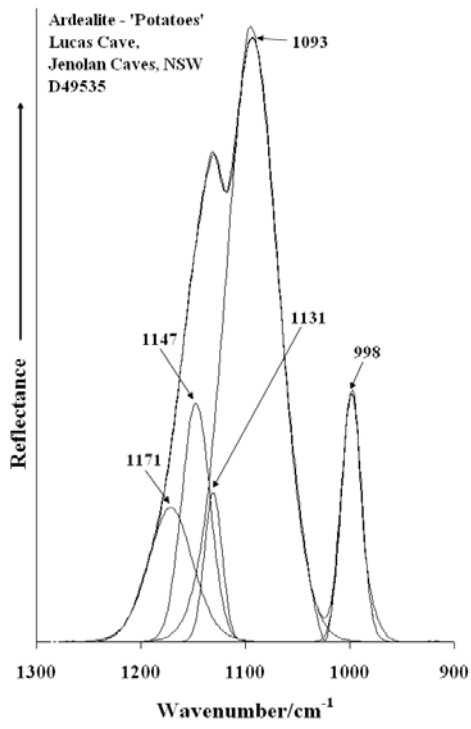


Figure 4a

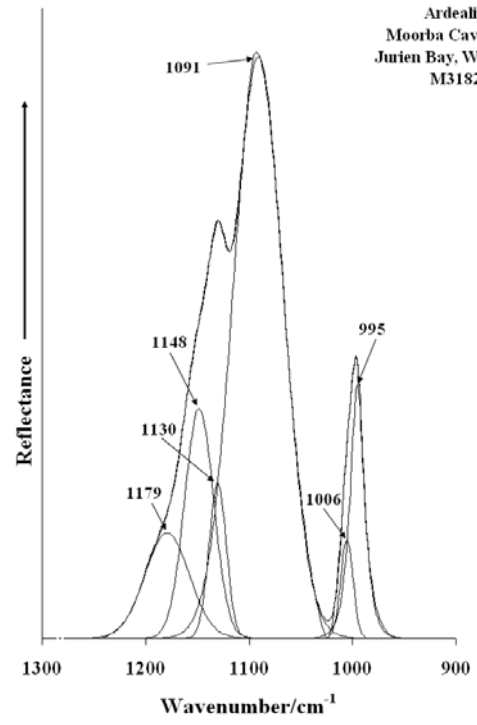


Figure 4b

299

300

301

302

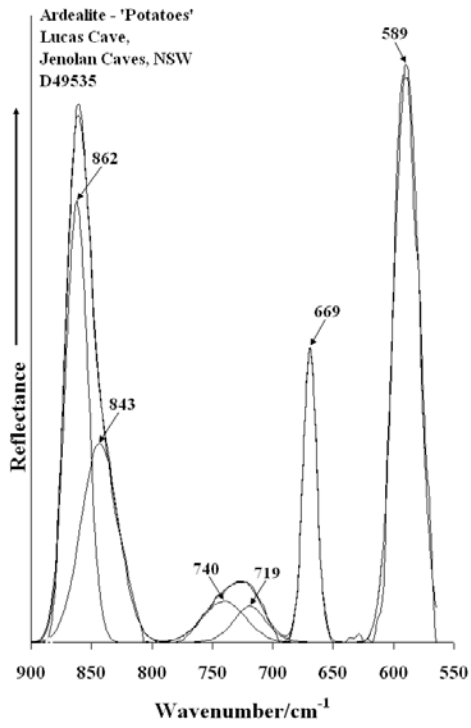


Figure 5a

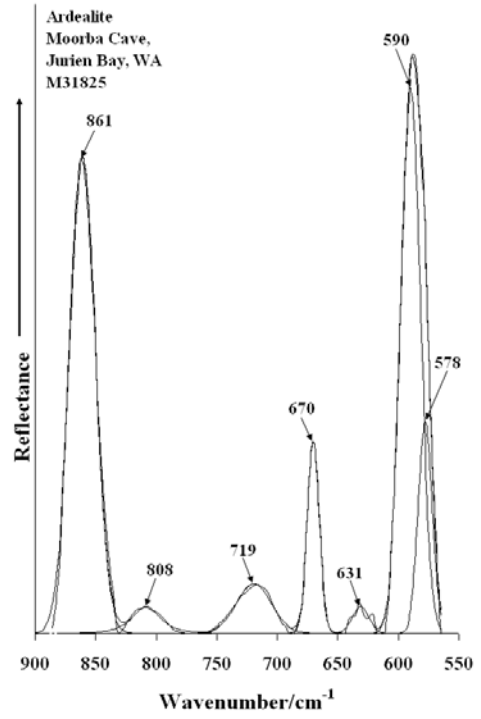


Figure 5b

303

304

305

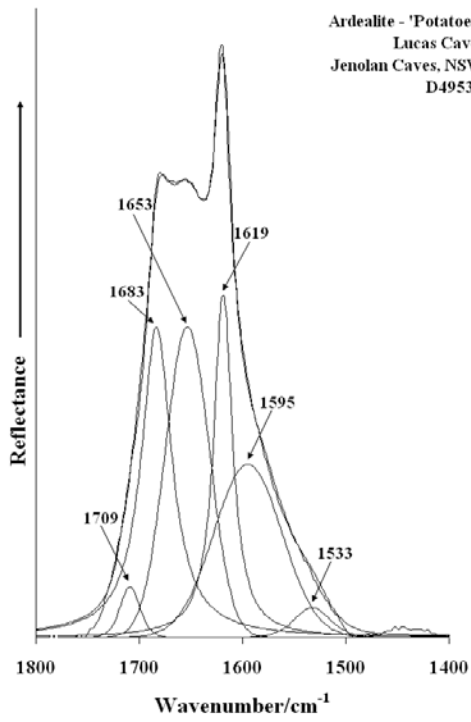


Figure 6a

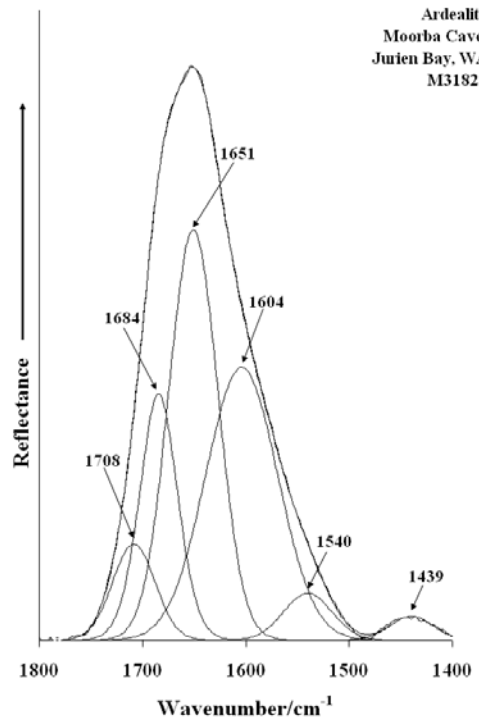


Figure 6b

306

307

308

309

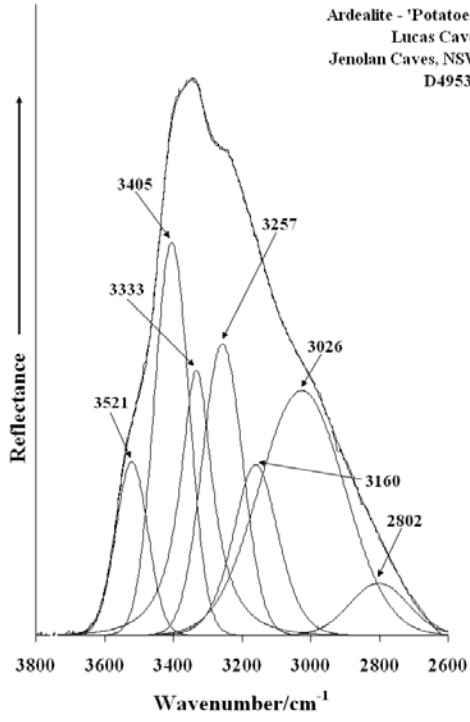


Figure 7a

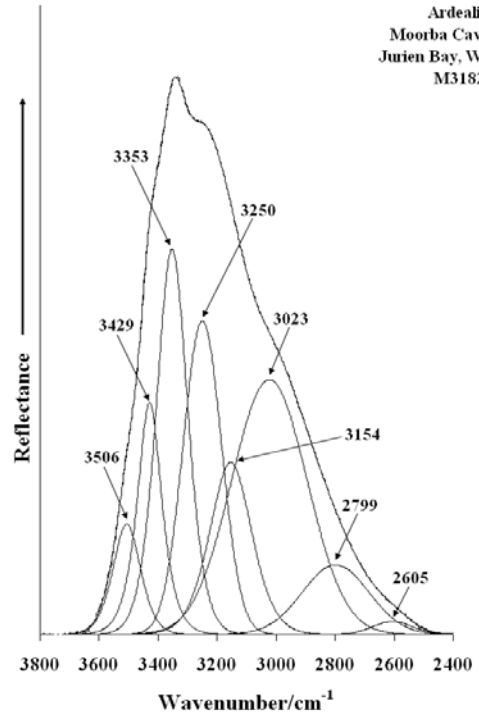


Figure 7b

310

311